Evaluation of a commercial high resistance bridge and methods to improve its precision

Metrol. Meas. Syst., Vol. 29 (2022) No. 4, pp. 701–718
DOI: 10.24425/mms.2022.142276

PAN POLSKA AKADEMIA NAUK

METROLOGY AND MEASUREMENT SYSTEMS
Index 330930, ISSN 0860-8229
www.metrology.wat.edu.pl

M&MS

EVALUATION OF A COMMERCIAL HIGH RESISTANCE BRIDGE AND METHODS TO IMPROVE ITS PRECISION

Iulian Mihai, Pier Paolo Capra, Flavio Galliana

National Institute of Metrological Research, Applied Metrology and Engineering Department, Str. delle Cacce 91, 10135 Turin, Italy (*i.mihai@inrim.it*, *p.capra@inrim.it*, ✉*f.galliana@inrim.it*, +39 011 391 9336)

Abstract

At the National Institute of Metrological Research (INRIM) an evaluation of a commercial dual source high resistance bridge has been performed. Its two main measurement modes (single measurements and multiple measurements) have been investigated. The best settle time of a 10:1 measurement of high resistance ratio has been estimated to be about three times the time constant of the circuit involving the resistors. This constant, in turn, depends on the highest value resistor. By means of mathematical estimators, suitable numbers of the readings of the detector have been established in order to minimize noises. A compatibility test at 100 TΩ has shown that the best precision of the commercial bridge is achieved utilizing the multiple measurements mode with the auto update function. This mode also allows the characterization of a resistor as a function of the settle time. This characterization can be useful for the owner of the resistor who can request the laboratory to perform the calibration of the resistor with the settle time which is necessary for him.

Keywords: high resistance measurements, dual source bridge (DSB), settle-time, measurement uncertainty, compatibility test, measurement noise.

1. Introduction

High dc electrical resistance measurements are widespread from *National Measurement Institutes* (NMIs) that perform high level calibrations, down to industrial laboratories and applications. Ultra-high resistance measurements are needed for calibration of low currents at 1 pA level or below (pico-femto ammeters) and for ion-beam applications. In the industrial framework, high resistance measurements are necessary in sensors applications and to evaluate insulation resistances and volume/surface resistivity. Since the eighties, methods for calibration of high value resistors have been realized [1–8]. The most used is the *dual source bridge* (DSB) method consisting in two dc voltage calibrators in two arms of a Wheatstone bridge (Fig. 1).

Voltages V_x and V_s are respectively applied to the resistor under calibration R_x and to the standard resistor R_s. The voltage ratio is set up so that the currents in R_s and in R_x are in opposition and the detector measures their difference. The bridge is balanced when this difference is null.

Article history: received May 24, 2022; revised July 2, 2022; accepted July 11, 2022; available online September 16, 2022.

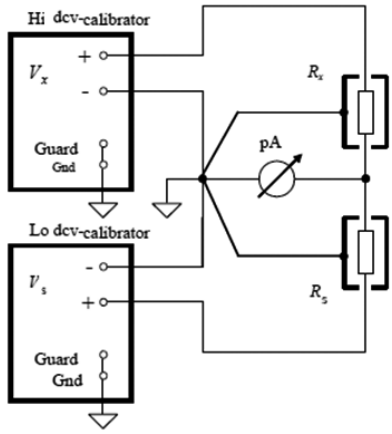

Fig. 1. Scheme of the DSB measurement method on which the commerciale bridge is based.

As the perfect balance cannot be achieved, it is approached as close as possible adjusting V_s and fixing V_x. The residual unbalance current is then measured by the detector. The measurement is made at both polarities. At the bridge balance the following equation is valid:

$$r = \frac{R_x}{R_s} = -\frac{V_x}{V_s} \,. \tag{1}$$

The unbalance is the difference (in dc current) from the ideal bridge balance that is verified when a perfectly nulled current is present at the detector when both the resistors are supplied. The resistance value for a slight unbalance is evaluated according to [9] par. 4.1. As a null detector, alternatively to a picoammeter, a nanovoltmeter can be used according to the R_x value [8]. The nanovoltmeter measures the voltage difference instead of the current difference to detect the bridge balance. At the *National Institute of Metrological Research* (INRIM), besides the DSB method, mainly used for calibration of resistors from 1 TΩ to 100 TΩ, another method based on a dc voltage calibrator and a *digital multimeter* (DMM) is also used for calibrations from 1 GΩ to 1 TΩ [4,6,7]. With these two methods, INRIM participated with satisfactory results in the EURAMET.EM-S32 supplementary comparison, resistance standards at 1 TΩ and 100 TΩ and in the key comparison CCEMK2 of resistance standards at 10 MΩ and 1 GΩ [9, 10]. Recently, papers [11, 12] have respectively reported further advances of the DSB method and a comparison of different methods in the 1 PΩ–100 PΩ range. In [12] it is also stated that the DSB method is limited to 1 PΩ. To expedite the calibration activity for external customers, INRIM also acquired a commercial automatic high resistance DSB bridge operating, according to the manufacturer specifications, from 100 kΩ to 10 PΩ [13]. Its software provides at the end of the measurements a file giving ratio and resistance values, standard deviation and an estimated uncertainty of R_x. This sort of calibration report immediately available is much appreciated in industrial applications. The characterization and validation process of the commercial bridge has been underway at INRIM for some years consisting mainly in comparing the measurements of this bridge with those made with the other two validated methods. Instead, the aim of the present work has been a deep investigation of its measurement modes. The novelty lies in the use of statistical tools to determine the appropriate number of the readings of the detector in order to minimize noises, in the identification of the measurement mode offering the best precision and in the characterization of the resistors as a function of the settle time (*st*) which are deemed necessary by the prospective users of the resistors.

Metrol. Meas. Syst., Vol. 29 (2022), No. 4, pp. 701–718
DOI: 10.24425/mms.2022.142276

2. The high resistance commercial bridge

The instrument in its initial version was provided to INRIM with two pairs of measurement cables (RG58). It is now located in a shielded room placed inside a thermo-regulated laboratory. It is connected to an independent ground potential and controlled through an IEEE488 interface linked to a computer outside the shielded room. The bridge is equipped with two dc Transmille 3000A voltage calibrators and with a Keithley 6514 picoammeter [14] as a null detector. Also, the Keithley 6517 picoammeter [15] can be managed by the bridge and its software. The bridge allows also a direct measurement mode by means of voltammeter measurements. This mode allows a prompt evaluation of a resistor value, of its settle time, the measure of leakage and insulation resistances of cables. Another useful feature of the instrument is the possibility to calibrate the two dc voltage calibrators by comparison with a calibrated HP 3458A *digital multimeter* (DMM) by means of an automatic procedure. As suggested by INRIM, an updated version of the bridge software [16] takes into account these calibration results in the following calibrations of resistors for both bridge and voltammeter measurement modes. The precision of the voltammeter mode is further increased by calibrating the picoammeter as well.

2.1. Bridge modes: single and multiple measurements

The software of the commercial bridge offers two ratio measurement modes *i.e.* single measurement and multiple measurements. With the first one, the bridge performs measurements sets in a specific ratio R_x/R_s at a single voltage. The operator has to set only a few parameters, namely, the nominal (or estimated) value of R_x, the measurement voltage, the settle time, the number of readings by the detector, the total number of measurements, the value and uncertainty of R_s, the unbalance window, the number of measurements (statistics) with which the software estimates the value and the uncertainty of R_x. The unbalance window represents the closeness to the perfect bridge balance determining the current at which the bridge stops adjusting V_s. Before the real comparison, an initial test tries to achieve the balance starting from the unbalance window set by the operator. If the balance is not achieved, the program tries again doubling the unbalance window. This test is performed three times after which if no balance is achieved the program stops. If a balance is achieved, the program carries out the measurements, first with positive polarity and then with reversed polarity. The measurements of both polarities are averaged to calculate the values of the ratio and of R_x. In the setting of the measurement parameters for a calibration, the operator does not know the value of the resistor under calibration and the value of the standard resistor is known with a large uncertainty. In fact, being both resistors of ultra-high value, they can have values up to ±20% different from their nominal ones. Therefore, the operator sets the nominal voltages corresponding to the nominal ratio of the resistors under comparison and has to set an unbalance with which the bridge software has to find the best voltages corresponding to the real ratio value R_x/R_s. When it is necessary to evaluate the for example the voltage dependence of R_x, the multiple measurements mode is suitable. This mode consists in programmed multiple measurement sessions, with the same or different parameters as voltages, settle times, number of measurements *etc*. In this mode, an Auto-Update function is available in which the R_x value is automatically updated during each session. From the second session, the starting value of R_x is that evaluated in the previous session. Increasing the settle time at each session, for example starting in the first one from half the time constant τ of R_x (see next paragraph) and utilizing τ multiples in the following sessions, the updating of the R_x value allows to reduce the unbalance window at each session. In this way, the ideal bridge balance is approached as close as possible because at each step the residual current at the detector is lowered approaching the ideal balance

of the bridge for which the current at the detector should be null. By means of this iterative mode, investigations to improve the performance of the commercial bridge were made. In Table 1, the calibration results of a 100 TΩ resistor vs. a 10 TΩ one are reported. These two resistors, manufactured by *Measurement International* (MI), model MI 9331G constitute a single resistive element.

Table 1. R_x values and standard deviations in an iterative process of four sessions at different settle times and for a lower number of measurements in the first sessions. The ratio 1:10 involves a 10 TΩ resistor and a 100 TΩ one.

Voltage	**Session**	**No meas.**	***st* (s)**	**R_x (TΩ)**	**Standard deviation ($\times 10^{-4}$)**
1000 V	0	–	0	100	–
	1	5	$300 \cong \tau/2$	91.49	4.9
	2	5	$600 \cong \tau$	91.56	4.7
	3	5	$1200 \cong 2\tau$	91.61	4.3
	4	50	$1800 \cong 3\tau$	91.99	1.6
500 V	5	5	300	95.69	12.8
	6	5	600	95.83	12.6
	7	5	1200	95.87	6.7
	8	50	1800	95.94	2.9

In the session 0, the bridge performs a preliminary balance taking into account the nominal value of R_x. Then, for each session, the R_x value is updated and progressively approaches the best estimate. This is observable from the decreasing of the standard deviation at each session. The updating process restarts with changing the voltage. In Fig. 2 the R_x values at 500 V along with the uncertainty bars corresponding to the standard deviation are shown. As the standard deviation becomes smaller at each session, so does the total uncertainty.

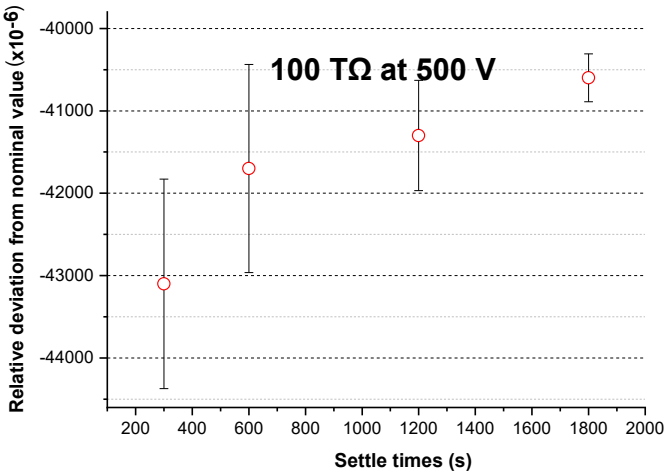

Fig. 2. Sequence of the R_x values at 500 V with the uncertainty bars corresponding to the standard deviation.

Metrol. Meas. Syst., Vol. 29 (2022), No. 4, pp. 701–718
DOI: 10.24425/mms.2022.142276

2.2. Best values of the settle time

The identification of suitable settle times of a high resistance ratio measurement is important because measuring for longer times could be counterproductive as the random drift could become dominant. The unbalance windows and settle times suggested by the manufacturer increase as increases the value of the resistances under comparison. This is valid for all resistors but mainly for those made with a single resistive element. The manufacturer recommends for these resistors a settle time between 600 s and 2000 s and an unbalance of 2% for the ratio 10 TΩ–100 TΩ at 1000 V. Our measurements in this ratio were performed at different settle times in order to find the one to achieve the best measurement precision and to compare with the settle times suggested by the manufacturer. As time constant τ of an RC circuit is the time to charge the capacitance of the circuit to the 63.2% of its total charge, the R_x value vs. the time t depends on the Euler number, with an increasing exponential behaviour:

$$\frac{\Delta R(t)}{R} = \frac{R_{\max}}{R} - \frac{(R_{\max} - R_{\min})}{R} e^{-t/\tau}, \tag{2}$$

where R, $R_{\max}$ and $R_{\min}$ are respectively the nominal, the maximum and minimum R_x values obtained in a measurement session. For long measurement times, ($> 3\tau$), undesired effects such as the drift of the calibrators or resistance variations due to possible temperature changes can occur affecting the measurement precision. It is then appropriate to measure with a settle time no longer than 3τ.

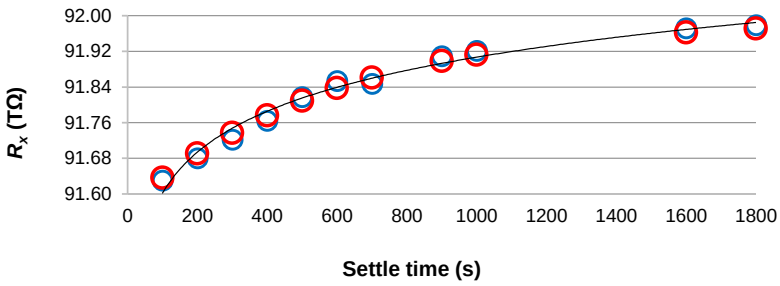

Fig. 3. R_x value as function of the settle time for the 10 TΩ–100 TΩ ratio at 1000 V. In blue, the measured values while in red those estimated with the (2) are respectively shown.

All the differences between the measured R_x values and those estimated with (2) were within the ratios uncertainties. Since the capacitance of the measurement system is constant, from our experimental results, the time constant τ in this 10:1 ratio can be obtained as R_x function:

$$\tau \cong 13 \cdot e^{\frac{\ln(R_x)}{3}}. \tag{3}$$

Therefore, the best settle time of a high resistance ratio has been estimated to be about three times the time constant of the resistor circuit, which, in turn, mainly depends on the highest value resistor. In Table 2, examples of the settle times suggested by the manufacturer, given as generic and wide intervals [16], are compared with the time constant τ obtained with the (3) and with those obtained experimentally.

Table 2. Settle times suggested by the manufacturer compared with the evaluated time constant with the (3) and with experimental values.

Ratios	V_x	**Manufacturer settle time**	**Evaluated** τ	**Experimental best** $st \cong 3\tau$ **(s)**
1 TΩ : 10 TΩ	1000 V	200 s – 1200 s	280 s	840
10 TΩ : 100 TΩ	1000 V	600 s – 2000 s	603 s	1800

3. Noise critical issues

Although the current read by the detector is progressively reduced in an iterative process, it is not nulled. Since the noise due to electrostatic interference can occur mainly at the 100 TΩ level or higher, a detector with better resolution and lower noise sensitivity than the Keithley 6514, with which the commercial bridge is usually equipped, should be used. A limit example to show the noise effect was made comparing a 100 TΩ resistor and a 1 PΩ one. A measurement sequence at settle times from 600 s down to 30 s was set. The measurements were made without and with the resistors. The results are shown in Table 3. In both cases, the initial value of R_x was set to the nominal value. R_x values are expressed in terms of relative deviation from the nominal value[1].

Table 3. Measurement results of the ratio 100 TΩ–1 PΩ at different settle times with and without the resistors.

1000 V	**Without resistors**		**With resistors**	
st (s)	R_x ($\times 10^{-4}$)	St. dv. ($\times 10^{-4}$)	R_x ($\times 10^{-2}$)	St. dv. ($\times 10^{-4}$)
600	–0.4	5.9	22.2	73
300	5.5	4.6	25.1	72
120	10.9	4.8	28.9	88
60	16.9	4.8	41.0	95
30	28.4	4.3	66.3	117

In the first case, the bridge was balanced without detecting the absence of the resistors, providing even the R_x values. Presumably in this situation the bridge measured the air resistance. In addition, the standard deviation for these measurements was lower than that of the measurements with the resistors connected. Instead, the measurements without the resistors were not possible changing the detector *i.e.* inserting the Keithley 6517B due to its higher resolution. In fact, the program of the bridge always stopped after the preliminary measurement, presumably because of the detection by this more sensitive detector of currents higher than those set by the bridge software corresponding to the unbalance window. The bridge is affected by a basic noise. The cable noise instead is due mainly to the insulation but also to electromagnetic fields, triboelectric effect, static electricity. These noises cause measurement errors at the detector impairing the calibration activity. Analysing the measurements without the resistors, the standard deviation values are due to a threshold noise hard to further reduce even with the auto update function. This noise can be lowered only investigating its sources. The higher standard deviation of the measurements with the resistors is due to the addition of the intrinsic noises caused by the resistors themselves and, presumably, to the too short settle times. Nevertheless, the resistors are only affected by the

[1]The value of R_x expressed in relative deviation from its nominal value (for example in $\times 10^{-4}$) is calculated as: $\frac{[R_{x\_meas}(T\Omega) - R_{x\_nom}(T\Omega)]}{R_{x\_nom}(T\Omega)} \times 10^4$

Metrol. Meas. Syst., Vol. 29 (2022), No. 4, pp. 701–718
DOI: 10.24425/mms.2022.142276

Johnson noise. The measurement circuit can be affected instead by low frequency electromagnetic noises. To ensure that the overall noise of the measurement is only due to the intrinsic noise of the resistors, the measurements were analysed with alternative mathematical estimators to identify noise sources.

3.1. Analysis of the noises at the detector of the commercial bridge

The first compatibility test of the measurements with the commercial bridge (used only in single measurements mode) with those made with the two INRIM validated methods for high resistance was performed calibrating four high value resistors from 10 GΩ to 10 TΩ with satisfactory results [17], while in the second one [18] the compatibility was achieved also at 100 TΩ. Unfortunately, the test failed at 1 PΩ when the measurements carried out by the INRIM DSB bridge [4, 6, 7] and by the commercial bridge were both affected by hard noises. Typical noises in modern measurement instrumentation are the white noise and the $1/f$ noise due to the electronics. Mathematical estimators as the *Allan variance* (AV), the *overlapping Allan variance* (OAV), and the *power spectral density* (PSD), widespread in time and frequency metrology, were used in the past to improve the precision of electrical voltage and resistance measurements and to solve noise problems [19–22]. To evaluate the noises in the current measured by the detector, an analysis of the power spectrum of the readings of the detector was made. On the bridge arms, resistors with known value were connected. The analysis was carried out by means of a *fast Fourier transform* (FFT) analyser connected with the detector output. The goal was to find the white noise regime for which the measurements can be considered independent and their distribution characterized by the standard deviation of the mean. For correlated data, this statement is no longer valid [19, 20]. Correlated data are those in which the measurements are affected, for example, by drift (not random). Correlation influences the variance of the mean and the correct expression for the standard deviation of the mean should include among observations the effect of correlations.

3.2. Analysis by means of the power spectral density

The detector and its output circuit can be represented as a unidirectional system with a transfer function H_D with input signal $x(t)$. The output signal $y(t)$ is a convolution of $x(t)$ and H_D. An evaluation of the intrinsic noise as the $1/f$ one, mainly due to the DC calibrators, was performed by means of the setup of Fig. 4. The transfer function $H_D(f)$ of the system is given by the transfer functions of the detector and of its output circuit. This last one depends on the RC low filter of the detector at its output circuit.

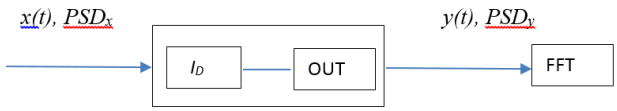

Fig. 4. Setup to evaluate the noises at the detector whose output circuit is connected to a FFT analyser.

For a function $y(t)$, periodical in the interval t_T, the *Direct Fourier Transform* (DFT) $F_y(f, t_T)$ is given by:

$$F_y(f, t_T) = \int_0^{t_T} y(t) e^{-j(2\pi f t)} \, \mathrm{d}t, \tag{4}$$

while the PSD(f) is given by:

$$\mathrm{PSD}_y(f) = \lim_{t_T \to \infty} \frac{2}{t_T} \left| F_y\,(f, t_T) \right|^2 . \tag{5}$$

The PSD for the unidirectional system in Fig. 5 can be written as:

$$\mathrm{PSD}_y(f) = S_y(f) = |H_D(f)|^2\, \mathrm{PSD}_X(f), \tag{6}$$

where $\mathrm{PSD}_X(f)$ and $\mathrm{PSD}_y(f)$ are the PSDs respectively at the input and at the detector output circuit. The $\mathrm{PSD}_y(f)$ of a time series $\overline{y}_I(\tau_0)$ can be modelled as:

$$\mathrm{PSD}(f) = \sum_{i=-2}^{2} \eta_i f^i, \tag{7}$$

where the intensity coefficient η_i and the index i depend on the noise type[2].

The AV $= \sigma_y^2(\tau)$ and the PSD(f) corresponding to the two types of low frequency noise are shown in Table 4.

Table 4. PSD and AV of the two types of low frequency noise.

Type	**PSD**(f)	**AV**(τ)[3]
white noise	η_0	$\frac{\eta_0}{2\tau}$
$1/f$ noise	$\eta_{-1} f^{-1}$	$2\eta_{-1} \ln(2)$

For the white noise, AV is proportional to τ^{-1} while the PSD is constant for the white noise and inversely proportional to the frequency for the $1/f$ noise. To analyze the noise types at the detector, the input current at the detector was converted to ±2 V voltage at the 2V detector output. This voltage was acquired by a Tektronix TDS 3032 digital FFT analyzer. The distortion due to the output low pass filter of the detector was investigated to correctly estimate the variance of the mean $\sigma(\overline{y_{(t)}})$ of the current measurements. Being $y(t)$ the function of the detector readings, the following relation is valid [23]:

$$\sigma^2\,(\overline{y_{\mathrm{out}}}) \approx \frac{\sigma^2\,(y_{\mathrm{out}})}{n} \sqrt{k}\,, \tag{8}$$

where,

- $k = \left\lceil \dfrac{1 + e^{-4B\tau_0}}{1 - e^{-4B\tau_0}} \right\rceil$;
- y_{out} are the detector readings;
- B is the bandwidth of the low pass filter;
- τ_0 is the sample at the same time interval;

$\sigma^2\,(y_{\mathrm{out}})$ is calculated by means of the statistical variance of n readings. In our case $B\tau_0 \gg 1$ meaning that the low pass filter does not introduce measurement distortion as it is faster compared to the variation of the output voltage. Elaborating the readings of the detector with the Stable32 software [24], the PSDs were determined in two measurement series for the ratio 10 TΩ–100 TΩ. The involved resistors were the10 TΩ MI model MI 9331G with a single resistive element and the 100 TΩ Guildline (Gdl) model 9337 100 T based on a resistor network. The measurements were made at 1000 V at both polarities. The obtained PSDs are shown respectively in Figs. 5 and 6.

[2]Typical values of i are 0 for the white noise and −1 for the $1/f$ noise.

[3]This τ is not the time constant of the resistor but is the time interval of the Allan deviation and PSD created by the Stable32software (see Figs. 7 and 8).

Metrol. Meas. Syst., Vol. 29 (2022), No. 4, pp. 701–718
DOI: 10.24425/mms.2022.142276

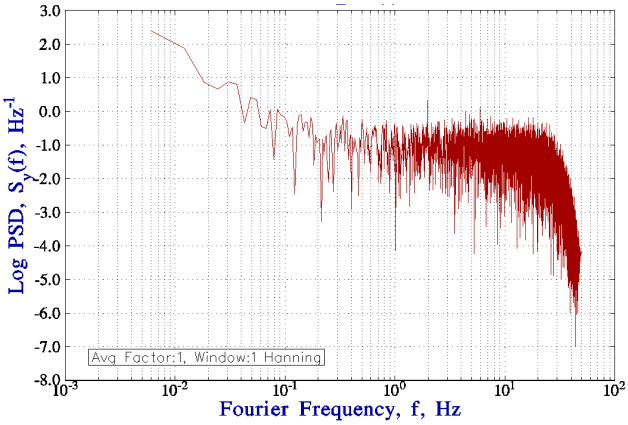

Fig. 5. PSD for the comparison 10 TΩ MI:100 TΩ Gdl with positive polarity at 1000 V, from 0 Hz to 50 Hz.

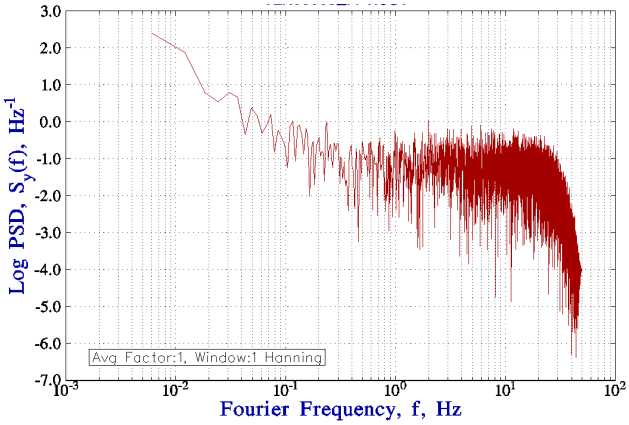

Fig. 6. PSD for the comparison 10 TΩ MI:100 TΩ Gdl with negative polarity at 1000 V, from 0 Hz to 50 Hz.

The Stable32 software was also used to compute the Allan deviation (AD = AV root square) at the time interval of 0.01 s for the same raw data, obtained with the FFT analyzer (respectively for positive and negative voltage polarity). The results are shown in Figs. 7 and 8.

According to the detector manual for the Keithley 6514 [14], par. 6.6, the noise reaches the minimum at integration times from about 20 ms to 200 ms, then this detector is optimized for a readings rate corresponding to this range. At these speeds the detector makes corrections of its own internal drift and still is fast enough to settle a step response. The software of the commercial bridge sets the detector at 1 PLC corresponding to the reading rate of 20 ms. To obtain a suitable number of readings with the detector, the mean time τ[4] at the minimum value of the AD (in the white noise regime) has to be divided by 20 ms. In Table 5 the values for the ratio 10 TΩ MI:100 TΩ Gdl are shown.

[4]This τ is not the time constant of the resistor but the same reported in Table 4.

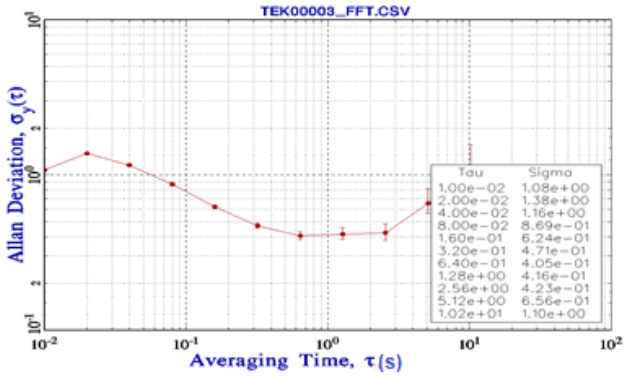

Fig. 7. AD for the comparison 10 TΩ MI:100 TΩ Gdl with positive polarity at 1000 V.

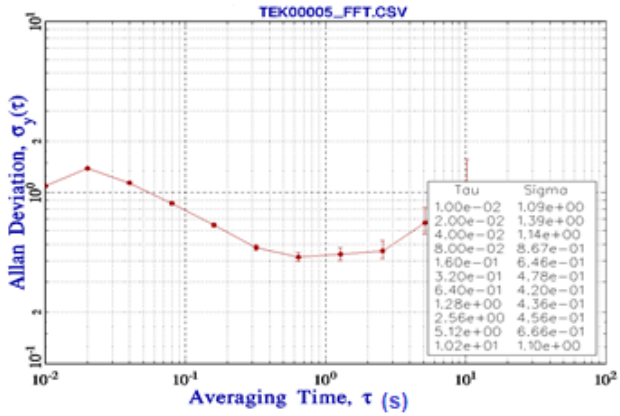

Fig. 8. AD for the comparison 10 TΩ MI:100 TΩ Gdl with negative polarity at 1000 V.

Table 5. Conversion from the minimum AD to the number of detector readings for the ratio 1:10.

Voltage	**AD = $\sigma_y(\tau)$ (mV)**	**τ (s)**	**Number of detector readings (NPLC[5] : 20 ms)**
0	0.37	5.12	256[6]
250	0.43	1.28	64
500	0.39	0.64	32
750	0.41	0.64	32
1000	0.40	0.64	32

[5]It selects the medium integration time (1 PLC) and sets display resolution to 5½-digit resolution. MED rate is selected when a compromise between noise performance and speed is acceptable.

[6]The number of electrometer readings is limited (by the software version 2.2.0) to 100 readings. DIGITAL FILTER: averaging is selectable from 2 to 100 readings.

Metrol. Meas. Syst., Vol. 29 (2022), No. 4, pp. 701–718
DOI: 10.24425/mms.2022.142276

4. Insights on the best performance of the commercial bridge

To find the best performance of the commercial bridge and to gain the compatibility with reference values, the measurements of the previous ratio 10 TΩ MI–100 TΩ Gdl were made both in single measurements mode (quick mode) and in multiple measurements mode. For both modes, a 600 s time constant was used.

4.1. Measurements at constant settle time

In the first measurement process, fifty ratio measurements (for both polarities) at a constant settle time for the whole comparison were made. This process was performed at 250 V, 500 V, 750 V and 1000 V obtaining the mean ratios r_{A0}. The voltages 25 V, 50 V, 75 V and 100 V on R_s respectively for the sessions from 1 to 4 were constant. The flow-chart of the process is shown in Fig. 9 with R_x initial value was set as the nominal value.

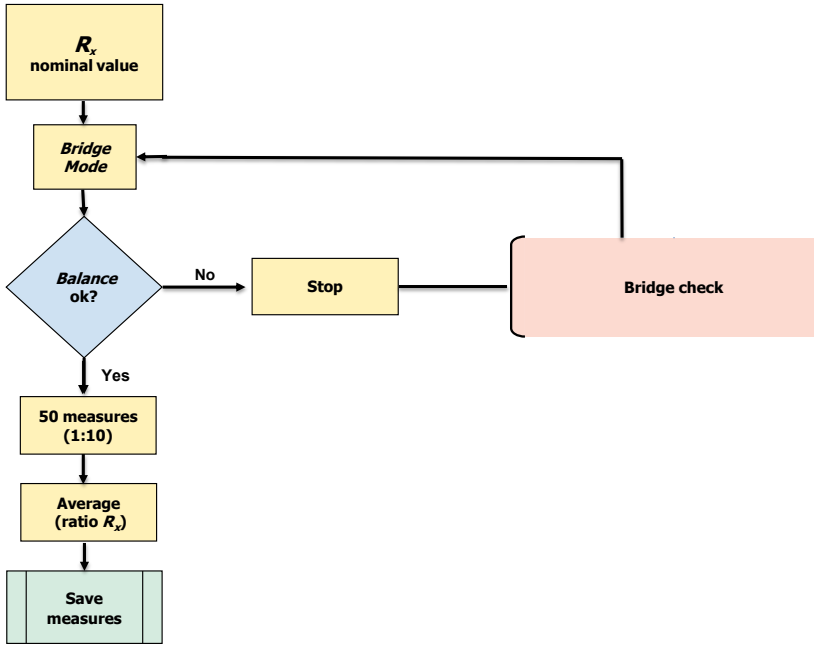

Fig. 9. Flow chart of the measurement process at the constant settle time.

4.2. Measurements at variable settle times

In the second measurement process four sessions were made at each voltage for different settle times and with a progressively reduced measurement number. The R_x value was obtained by means of the Auto update function. In the last three sessions, although maintaining the maximum unbalance value, the real unbalance was automatically reduced. The results for the second process were the ratios r_{A1}, r_{A2}, r_{A3} and r_{A4}. The voltages 25 V, 50 V, 75 V and 100 V on R_s respectively changed according to the R_x updated values. The flow-chart of the process is shown in Fig. 10 again with R_x initial value set as the nominal value.

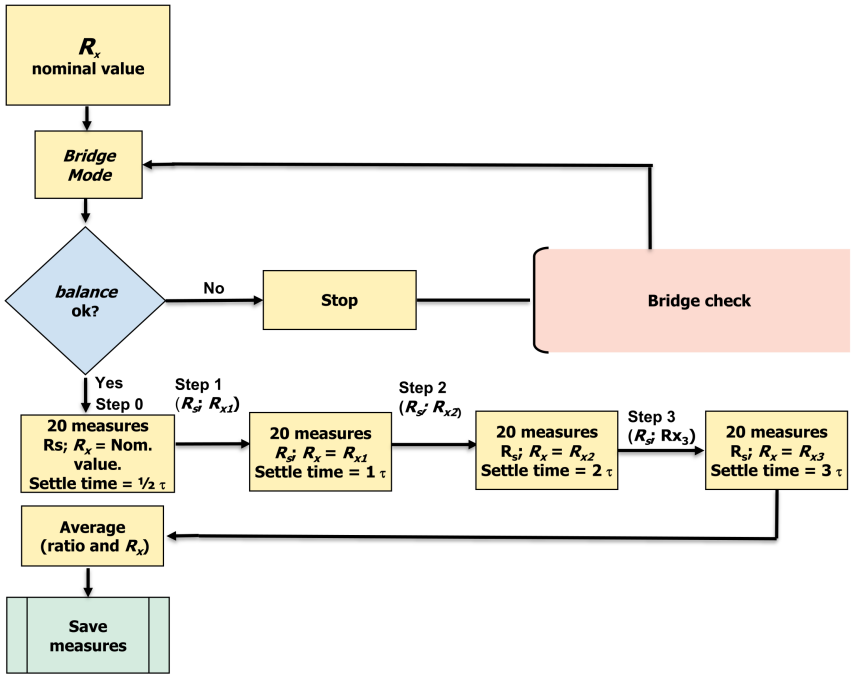

Fig. 10. Flow chart of the measurent process with variable settle times.

4.3. Measurement results

In Table 6, the results with the two modes are reported again expressed as relative deviation from the nominal value (see Footnote[1]). In the first four rows the measurement results at the constant settle time are reported, while in the successive rows the measurement results at increasing settle times (from ½ τ to 3 τ) for each voltage are shown respectively. In the last two columns, the standard deviation of the mean of the measurements (uncorrelated) [25] and the relative deviations between the measurements made at 3 τ respectively with the constant settle time and after the iterative process are respectively reported. A considerable difference can be observed between the measurement at 3τ between the two modes (see also Fig. 11).

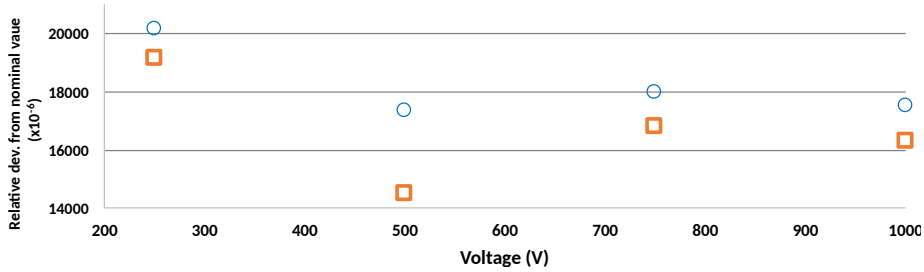

Fig. 11. Relative deviation of the measurement values at settle time 3 τ measured at the constant settle time (blue circles) and with the autoupdate process (orange dots).

The reason of these deviations will be further investigated with the manufacturer.

Metrol. Meas. Syst., Vol. 29 (2022), No. 4, pp. 701–718
DOI: 10.24425/mms.2022.142276

Table 6. Measurements of the ratio 10 TΩ MI (R_s) vs. 100 TΩ (R_x) Gdl at constant and variable settle times.

Comparison			**st**	**Unbalance**	**Voltage**	R_x	**sdvm**	**Δ modes**
number	Code		(s)	($\times 10^{-6}$)	(V)	($\times 10^{-4}$)	($\times 10^{-4}$)	($\times 10^{-4}$)
1	r_{A0}/250 V	3τ	1800	40001	250	4.5	6.8	
2	r_{A0}/500 V	3τ	1800	20001	500	1.6	4.0	
3	r_{A0}/750 V	3τ	1800	13334	750	2.2	3.4	
4	r_{A0}/1000 V	3τ	1800	10001	1000	17	2.5	
5	r_{A1}/250 V	$1/2\tau$	300	40001	250	2.5	13.2	
6	r_{A2}/250 V	1τ	600	40001	250	4.9	17.8	
7	r_{A3}/250 V	2τ	1200	40001	250	2.5	3.3	
8	r_{A4}/250 V	3τ	1800	40001	250	3.5	11.5	–9.9
9	r_{A1}/500 V	$1/2\tau$	300	20001	500	1.3	6.0	
10	r_{A2}/500 V	1τ	600	20001	500	2.5	6.2	
11	r_{A3}/500 V	2τ	1200	20001	500	1.8	1.5	
12	r_{A4}/500 V	3τ	1800	20001	500	–1.1	3.3	–27.9
13	r_{A1}/750 V	$1/2\tau$	300	13334	750	1.5	3.4	
14	r_{A2}/750 V	1τ	600	13334	750	1.1	2.9	
15	r_{A3}/750 V	2τ	1200	13334	750	1.8	0.9	
16	r_{A4}/750 V	3τ	1800	13334	750	1.1	4.9	–11.3
17	r_{A1}/1000 V	$1/2\tau$	300	10001	1000	1.3	3.1	
18	r_{A2}/1000 V	1τ	600	10001	1000	2.	1.9	
19	r_{A3}/1000 V	2τ	1200	10001	1000	1.5	0.8	
20	$r_{A4/}$1000 V	3τ	1800	10001	1000	0.5	2.5	–12.1

4.4. Compatibility test

A compatibility check between the values of the commercial bridge on the 100 TΩ resistor Gdl at 1000 V and the value given by the accredited laboratory operating at the Guildline company in Canada, was performed. The traceability of the INRIM measurements started from a 1 TΩ Guildline model 9337 resistor number 64486 calibrated with the two INRIM high resistance validated methods.

Within the comparison, three measurements using the commercial bridge were performed at INRIM:

- At settle time 3τ, r_{A0}/1000 V, after a process at the constant settle time;
- At settle time 3τ, r_{A4}/1000 V, after an iterative process with autoupdate function;
- At settle time 2τ r_{A3}/1000 V, at the lowest standard deviation of the mean.

Following a preliminary uncertainty budget of the measurements with the commercial bridge [18], an uncertainty budget according to [25] at 100 TΩ at 1000 V with autoupdate function (at 3τ) is reported in Table 7. The uncertainties for the other two measurements were obtained inserting their R_x noise values (*i.e.* standard deviation of the mean). The measurements with the commercial bridge at 100 TΩ are given in Table 8, expressed as relative deviation from the nominal value (see Footnote[1]), along with their expanded uncertainties. In the same table, also a measurement made with the INRIM DSB bridge is reported.

Table 7. Uncertainty budget for the calibration of the 100 TΩ resistor at 1000 V with the updating process (measurement code r_{A4}/1000 V) with the commercial bridge.

Uncertainty component	**Type**	**1σ ($\times 10^{-4}$)**
$R_{s\,\mathrm{cal}}$	Rect. B	2.10
$R_{s\,\mathrm{drift}}$	Rect. B	0.25
$R_{s\,\mathrm{temp}}$	Rect. B	0.50
$R_{x\,\mathrm{temp}}$	Rect. B	0.80
$R_{s\,V\,\mathrm{coeff}}$	Rect. B	0.02
Connections	Rect. B	0.50
Leakages	Rect. B	0.50
R_x noise	Rect. A[7]	1.04
Balance	Rect. B	0.5
Sensitivity	Rect. B	0.5
Meas. Stab.	Rect. B	0.50
Commercial bridge spec.	Rect. B	1.70
RSS u(R_x)		**3.05**

Table 8. Expanded uncertainties for the calibration of the 100 TΩ resistor at 1000 V with the updating process, at the constant settle time and with the best repeatability.

Measurement method	**R_x value ($\times 10^{-4}$)**	**R_x expanded uncertainty ($\times 10^{-4}$)**
With an autoupdate process	4.9	6.1
At constant settle time 3τ	17.0	7.6
With best standard deviation	15.2	5.9
Gdl certificate	–2.6	8.0
INRIM bridge	2.1	6.6

As uncertainty of the measurement with the INRIM DSB bridge, the approved *calibration measurement capability* (CMC) reported in the MRA[8] database at 100 TΩ (6.6×10^{-4}) was considered although the evaluated uncertainty in this case yielded lower results. Fig. 12 shows the agreement of the INRIM measurements (with both bridges) on the 100 TΩ resistor with the value provided by the calibration certificate number 18440 on 17 November 2021 issued by the Guildline laboratory.

5. Discussion

Observing Fig. 12, only the value of the commercial bridge at 3τ after the iterative process (blue circle) is compatible with the values of the Gdl certificate and of the INRIM DSB bridge. First of all, this value agrees for the progressive R_x update and for the increased standard

[7]This value was considered corresponding to a rectangular distribution observing that the measurements assumed a flat distribution presumably for the completion of the autoupdate process.

[8]The CIPM Mutual Recognition Arrangement (CIPM MRA) is the framework through which National Metrology Institutes demonstrate the international equivalence of their measurement standards and of their calibration certificates. The outcomes of the Arrangement are the internationally recognized Calibration and Measurement Capabilities (CMCs) of the participating institutes.

Metrol. Meas. Syst., Vol. 29 (2022), No. 4, pp. 701–718
DOI: 10.24425/mms.2022.142276

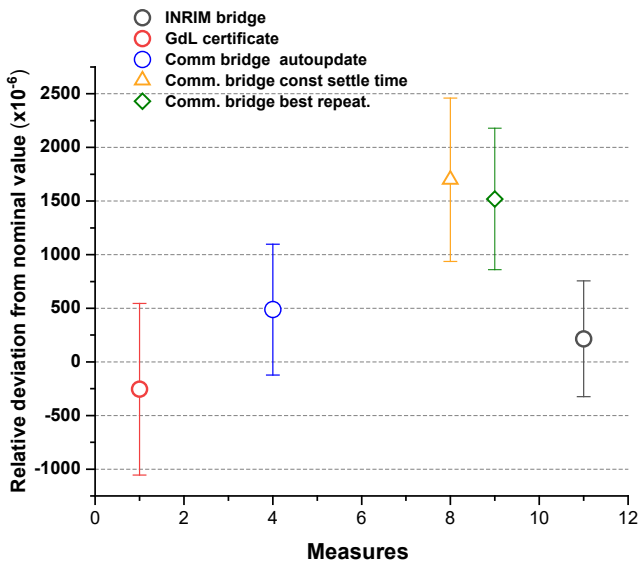

Fig. 12. Compatibility check among the measurements with the commercial bridge, with the INRIM DSB bridge and the value of the Guildline certificate of the 100 TΩ resistor. The uncertainty bars correspond to the expanded uncertainty at 95.5% confidence level.

deviation of the measurements causing a larger uncertainty contributing to the compatibility. This increased measurement spread was presumably due to the drift of the calibrators after such a long time (measurements at $1/2\tau$, τ, 2τ and 3τ). Secondly, the other two values with the commercial bridge were not compatible respectively for the lack of the R_x refinement process (measurement at constant settle time 3τ, orange triangle) and for the incomplete R_x updating process (measurement with the lowest standard deviation, green rhombus). Its lower standard deviation also reduced the total uncertainty contributing to the lack of compatibility with the values of the Gdl certificate and of the INRIM DSB bridge. Therefore, currently the commercial bridge cannot provide, at 100 TΩ level and with the single measurements mode, a high precision measurement, even with a suitable settle time (3τ). A better result can be achieved only with a longer measurement with the multiple measurements mode and the autoupdate function. However, the Guildline measurements were made five months before all INRIM ones. Drift and transport effect on the resistor may have occurred during this period

6. Conclusions

Currently, multiple measurements one with the autoupdate function performing measurement sessions with increased settle times seem to be the measurement mode of the commercial bridge offering the best precision for ultra-high resistance values. This process lasts several hours and it can be economically unsuitable for secondary or industrial laboratories that normally expect a prompt calibration value. Anyhow, considering the wider uncertainty needs of this kind of laboratories, also the results with the faster single measurements mode could be acceptable. For high-level laboratories or NMIs, extended measurement times are less economically harmful. On the other hand, a long measure could lead to a higher uncertainty for the increasing of the mea-

surements spread due to the possible drift of the calibrators. In addition, the auto update function allows the characterization of a resistor under calibration vs. the settle time. This characterization could be added to the calibration certificate. In this way, a potential user can find, or request, the value of the resistor itself corresponding to the settle time with which he needs to use it. Future aims of the work are:

- A repetition of the compatibility test, setting as initial value of R_x the value obtained from a preliminary measurement in the direct mode. This choice could expedite the achievement of an accurate R_x value and with a better repeatability;
- A repetition of the same test using a further software release of the commercial bridge recently provided by the manufacturer;
- A repetition of the measurements after replacing the RG58cables provided with the bridge with triaxial ones to verify if a higher shield level could improve the measurement precision and stability and reduce the noises;
- A triangular test consisting in the comparisons: 10 TΩ MI–100 TΩ Gdl at multiple voltages and settle times, 10 TΩ MI–100 TΩ MI at the same voltages and 100 TΩ MI–100 T Gdl to verify the results of the first two comparisons;
- A comparison between a 100 TΩ and a 1 PΩ Gdl resistors, both based on a resistor network, to verify whether the commercial bridge balance is achievable and if the experimental settle time is lower than that obtainable with the (3). This is because it was observed by means of voltammeter measurements that the settle time of high value resistors based on resistors network seems much shorter than that of high value resistors with a single resistance element.

References

[1] Henderson, L. C. (1987). A new technique for the automatic measurement of high value resistors. *Journal of Physics E: Scientific Instruments*, *20*(5), 492. https://doi.org/10.1088/0022-3735/20/5/002

[2] Jarrett, D. G. (1997). Automated guarded bridge for calibration of multimegohm standard resistors from 1 MΩ to 1 TΩ. *IEEE Transactions on Instrumentation and Measurement*, *46*(2), 325–328. https://doi.org/10.1109/19.571848

[3] Schumacher, B., Pesel, E., & Warnecke, P. (1999). Traceability of high-value resistance measurements at PTB. *Proceedings of the 9th International Metrology Conference*, France.

[4] Galliana, F., & Boella, G. (2000). The electrical DC resistance scale from 100 kΩ to 1 TΩ at IEN. *IEEE Transactions on Instrumentation and Measurement*, *49*(5) 959–964. https://doi.org/10.1109/19.872914

[5] Jarrett, D. G. (2001). Analysis of a dual-balance high-resistance bridge at 10 TΩ. *IEEE Transactions on Instrumentation and Measurement*, *50*(2), 249–254. https://doi.org/10.1109/19.918114

[6] Galliana, F., Capra, P. P., & Gasparotto, E. (2009). Metrological management of the high dc resistance scale at INRIM. *Measurement, 42*(2), 314–321. https://doi.org/10.1016/j.measurement.2008.07.002

[7] Galliana, F., Capra, P. P., & Gasparotto, E. (2011). Evaluation of Two Alternative Methods to Calibrate Ultrahigh Value Resistors at INRiM. *IEEE Transactions on Instrumentation and Measurement*, *60* (3), 965–970. https://doi.org/10.1109/TIM.2010.2060226

[8] Rietveld, G., & van der Beek, J. H. N. (2013). High-Ohmic Resistance Bridge with Voltage and Current Null Detection. *IEEE Transactions on Instrumentation and Measurement*, *62*(5), 1760–1765. https://doi.org/10.1109/TIM.2013.2250171

Metrol. Meas. Syst., Vol. 29 (2022), No. 4, pp. 701–718
DOI: 10.24425/mms.2022.142276

[9] Jeckelmann, B., van der Beek, J. H. N., Capra, P. P., Chrobok, P., Cirneanu, L., Dudek, E., & Vrabcek, P. (2013). Final report on supplementary comparison EURAMET. EM-S32: Comparison of resistance standards at 1 TΩ and 100 TΩ. *Metrologia*, *50*(1A), 01008. https://doi.org/10.1088/0026-1394/50/1A/01008

[10] Dziuba, R. F., & Jarrett, D. G. (2002). Final report on key comparison CCEMK2 of resistance standards at 10 MΩ and 1 GΩ. *Metrologia*, *39*(1A). https://doi.org/10.1088/0026-1394/39/1A/1

[11] Jarrett, D. G., Payagala, S. U., Kraft, M. E., & Yu, K. M. (2016, July). Third generation of adapted wheatstone bridge for high resistance measurements at NIST. In *2016 Conference on Precision Electromagnetic Measurements* (CPEM 2016) (pp. 1–2). IEEE. https://doi.org/10.1109/CPEM.2016.7540782

[12] Yu, K. M., Jarrett, D. G., Rigosi, A. F., Payagala, S. U., & Kraft, M. E. (2019). Comparison of Multiple Methods for Obtaining PΩ Resistances With Low Uncertainties. *IEEE Transactions on Instrumentation and Measurement*, *69*(5), 3729–3738. https://doi.org/10.1109/TIM.2019.2941036

[13] Measurement International. (2013). *Automated dual source high resistance bridge model 6600A* [Operator manual, rev. 2].

[14] Keithley Instruments, Inc. (2003). *Model 6514 System Electrometer Instruction Manual* [4th rev].

[15] Keithley Instruments, Inc. (2008). *Model 6517B System Electrometer User's Manual* [rev. A].

[16] Measurement International. (2019). *Automated dual source high resistance bridge model 6600A* [Operator manual, rev. 5].

[17] Galliana, F., Capra, P. P., & Gasparotto, E. (2015). Evaluation of the measurement capabilities of an high performance commercial high resistance bridge by means of the comparison with two validated high resistance measurement methods. In *17th International Congress of Metrology* (p. 10001). EDP Sciences. https://doi.org/10.1051/metrology/20150010001

[18] Galliana, F., Capra, P. P., & Mihai, I. (2020). Measurement comparison between a commercial high resistance bridge and validated systems at ultra-high resistance values. In *24th IMEKO TC4 International Symposium 22nd International Workshop on ADC and DAC Modelling and Testing IMEKO TC-4 2020* (pp. 379–383).

[19] Allan D. W. (1987). Should the classical variance be used as a basic measure in standards metrology? *IEEE Transactions on Instrumentation and Measurement, IM-36*(2), 646–654. https://doi.org/10.1109/TIM.1987.6312761

[20] Witt, T. J. (2001). Using the Allan variance and power spectral density to characterize DC nanovoltmeters. *IEEE Transactions on Instrumentation and Measurement*, *50*(2), 445–448. https://doi.org/10.1109/19.918162

[21] Mihai, I., & Reedtz, G. M. (2002, June). Optimisation of a potentiometric measurement system by calculation of the Allan variance. In *Conference Digest Conference on Precision Electromagnetic Measurements* (pp. 48–49). IEEE. https://doi.org/10.1109/CPEM.2002.1034713

[22] Mihai, I., & Reedtz, G. M. (2001). Using spectral analysis and Allan variance to characterize a potentiometric measurement system. *Proceedings Conference Celebrating the* 50^{th} *anniversary of the Romanian National Institute of Metrology*, Bucharest, Romania (pp. 555-560).

[23] Fletcher, N., & Witt, T. J. (2008, June). Some applications of times series analysis techniques to coaxial AC bridges. In *2008 Conference on Precision Electromagnetic Measurements Digest* (pp. 344–345). IEEE. https://doi.org/10.1109/CPEM.2008.4574794

[24] Hamilton Technical Services. (2008). *Stable32 User Manual*. http://www.stable32.com/

[25] Joint Committee for Guides in Metrology. (2008). *Evaluation of measurement data – Guide to the expression of uncertainty in measurement* (JCGM 100:2008). http://www.bipm.org/utils/common/documents/jcgm/JCGM_100_2008_E.pdf

Iulian Mihai received his M.Sc. degree in physics from the University of Bucharest in 1995, in metrology engineering from the Bucharest Polytechnic of in 1998 and his Ph.D. degree in metrology from Politecnico di Torino in 2004. In 1999 he joined Istituto Elettrotecnico Nazionale "Galileo Ferraris" (IEN), Torino, where he was involved in resistance measurements and the quantum Hall effect studies. From 2005 to 2018 he joined industrial laboratories on electrical and mechanical measurements. In 2019 he joined the National Institute of Metrological Research (INRIM) where he has performed precision high resistance measurements.

Flavio Galliana received his M.Sc. degree in physics from the Università degli Studi di Torino in 1991. In 1993 he joined the IEN, Torino, where he was involved in high resistance measurements and worked in Accreditation laboratories. Since 2006, at the NRIM, he has been involved in resistance measurements and in interlaboratory comparisons.

Pier Paolo Capra received his M.Sc. degree in physics from University of Torino in 1996 and his Ph.D. degree in metrology from Politecnico di Torino in 2012. In 1987, he joined the IEN. From 2006, at INRIM, he has been involved in dc voltage resistance precision measurements.